Weierstraß–Institut
für Angewandte Analysis und Stochastik

im Forschungsverbund Berlin e.V.

Preprint ISSN 0946 – 8633

A model of a general elastic curved rod

Anca Ignat[1], Jürgen Sprekels[2], Dan Tiba[2, 3]

submitted: 18th October 2000

[1] Faculty of Computer Science
University "Al. I. Cuza"
str. Berthelot 16
RO–6600 Iaşi
Romania
E-Mail: ancai@thor.infoiasi.ro

[2] Weierstrass Institute
for Applied Analysis
and Stochastics
Mohrenstrasse 39
D – 10117 Berlin
Germany
E-Mail: sprekels@wias-berlin.de
E-Mail: tiba@wias-berlin.de

[3] Institute of Mathematics
Romanian Academy
P. O. Box 1–764
RO–70700 Bucharest
Romania
E-Mail: dtiba@imar.ro

Preprint No. 613
Berlin 2000

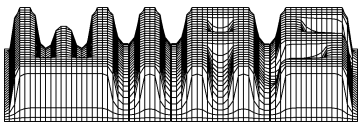

1991 *Mathematics Subject Classification.* 65N30, 34B60, 74B99.

Key words and phrases. Deformation of elastic rods, low geometrical regularity, variable cross sections.

Edited by
Weierstraß–Institut für Angewandte Analysis und Stochastik (WIAS)
Mohrenstraße 39
D — 10117 Berlin
Germany

Fax: + 49 30 2044975
E-Mail (X.400): c=de;a=d400-gw;p=WIAS-BERLIN;s=preprint
E-Mail (Internet): preprint@wias-berlin.de
World Wide Web: http://www.wias-berlin.de/

Abstract

We indicate a new approach to the deformation of three-dimensional curved rods with variable cross section. The model consists of a system of nine ordinary differential equations for which we prove existence and uniqueness via the coercivity of the associated bilinear form. From the geometrical point of view, we are using the Darboux frame or a new local frame requiring just a C^1-parametrization of the curve. Our model also describes the deformation occurring in the cross sections of the rod.

1 Introduction

This work is devoted to the study of three-dimensional curved rods with nonconstant thickness and with multiply connected cross section. Under the action of body forces and of (outside) surface tractions the rod will suffer deformations, and our approach allows to investigate deformations of variable cross sections as well.

The model we propose is expressed as a system of nine ODEs and is derived from the linear elasticity system under the minimal mechanical assumption that the transverse sections remain plane after the deformation, although their shape may change. We allow for shear and torsion, and even for (pointwise) degeneracy of the sections to dimension one. However, we underline that this last remark just means that our model does not impose other constraints than those coming from the validity requirements of the linear elasticity system.

The literature concerning curved rods is very rich, and the books of Trabucho and Viaño [19], Lagnese, Leugering and Schmidt [14], Antman [2] give a comprehensive overview of the existing results and methods, both in the stationary and the time-dependent cases. In the setting of asymptotic methods, we quote the recent paper by Jurak, Tambaca and Tutek [13] and the very recent work of Murat and Sili [15] announces the obtaining of an ODE model. The works of Reddy [17], Chenais and Paumier [8], Chapelle [7] discuss the "locking problem" for the numerical approximation of arches and curved rods. An explicit solution for the Kirchhoff–Love arches was found by Sprekels and Tiba [18], and a detailed examination of optimization questions is due to Ignat, Sprekels and Tiba [12].

An important ingredient in the study of curved rods is the description of their geometry and the choice of a local frame. While in the scientific literature the classical Frenet frame is, usually, taken into account, in this paper we consider other variants with the aim of relaxing the regularity assumptions or in connection with

certain applications. In the case of shells, such regularity questions were discussed by Blouza and Le Dret [4], Blouza [5].

In Section 2, we view the three-dimensional curve giving the line of centroids of the rod as lying on a fixed surface, and we use the Darboux frame, Cartan [6]. This approach requires a curve parametrization in $W^{2,\infty}$ and fits to the analysis of associated optimization problems where such a situation describes an important class of constraints. Section 3 introduces a direct method, based on a new choice of a Lipschitzian local frame for $W^{2,\infty}$ rods.

In all cases, we prove the coercivity of the corresponding bilinear form, and we obtain the existence and the uniqueness of the solution. In the last section, we present some numerical simulations based on our model, and we make a brief comparison with the already existing numerical results.

Finally, we point out that our way of working, by imposing the mechanical assumptions directly in the linear elasticity system, may be compared with the work of Delfour and Jiabin [11] in the case of shells.

2 The Darboux frame

Let $L > 0$ be given, and let $\omega(x_3) \subset I\!R^2$ be bounded domains, not necessarily simply connected, for any $x_3 \in [0, L]$. We assume that $\omega(x_3) \supset \omega$, a given open set in $I\!R^2$, such that

$$0 \;=\; \int\limits_{\omega} x_1 \, dx_1 \, dx_2 \;=\; \int\limits_{\omega} x_2 \, dx_1 \, dx_2 \;=\; \int\limits_{\omega} x_1 \, x_2 \, dx_1 \, dx_2 \, . \tag{2.1}$$

Hypothesis (2.1) on $\omega(x_3)$, $x_3 \in [0, L]$, is a slight relaxation of a similar condition used by Murat and Sili [15] and by Alvarez-Dios and Viaño [1].

We introduce the open set:

$$\Omega \;=\; \bigcup_{x_3 \in]0, L[} \Big(\omega(x_3) \times \{x_3\} \Big) \;\subset\; I\!R^3 \, . \tag{2.2}$$

The curved rod $\tilde{\Omega}$ is given as a transformation of Ω:

$$\begin{aligned} (x_1, x_2, x_3) \;=\; \bar{x} \;\in\; \Omega \;\mapsto\; F\,\bar{x} \;=\; \tilde{x} \;=\; (\tilde{x}_1, \tilde{x}_2, \tilde{x}_3) \\ =\; \bar{\theta}(x_3) \;+\; x_1\,\bar{n}(x_3) \;+\; x_2\,\bar{b}(x_3) \;\in\; \tilde{\Omega} \, , \quad \forall\; \bar{x} \;\in\; \Omega \, ; \end{aligned} \tag{2.3}$$

$$\tilde{\Omega} \;=\; \{\tilde{x} \;=\; F\,\bar{x} \, ; \, \bar{x} \;\in\; \Omega\} \, . \tag{2.4}$$

Here $\bar{\theta} \in W^{2,\infty}(0, L)^3$, with $\bar{\theta}''$ piecewise continuous is a three-dimensional curve, called the line of centroids, parametrized with respect to its arc length, and $\bar{n}(x_3)$, $\bar{b}(x_3) \in I\!R^3$ are some vectors for any $x_3 \in [0, L]$, which are different (in general)

from the normal and binormal vectors associated to the Frenet frame. In the sequel, for any vector $\bar{a} \in I\!R^3$, we shall denote by (a_1, a_2, a_3) its components.

We assume now that the curve $\bar{\theta}(\cdot)$ lies on a given surface S, defined by the equation

$$\phi(x_1, x_2, x_3) = 0 \tag{2.5}$$

with $\phi \in C^2(I\!R^3)$, that is,

$$\phi(\theta_1(x_3), \theta_2(x_3), \theta_3(x_3)) = 0 \quad \forall\, x_3 \in [0, L]. \tag{2.6}$$

We denote by $\bar{n}(x_3) = (n_1(x_3), n_2(x_3), n_3(x_3))$ a unit normal to S in the points $\bar{\theta}(x_3) \in S$, that is, $\alpha(x_3)\,\bar{n}(x_3) = \nabla\phi(\bar{\theta}(x_3))$ for some real mapping α. We also denote by $\bar{t}(x_3) = (\theta_1'(x_3), \theta_2'(x_3), \theta_3'(x_3))$ the unit tangent to the curve $\bar{\theta}(\cdot)$.

Finally, we choose the unit vector $\bar{b}(x_3) = \bar{t}(x_3) \wedge \bar{n}(x_3)$, the vectorial product between $\bar{t}$ and $\bar{n}$. Then, the local frame $(\bar{t}, \bar{n}, \bar{b})$ is positively oriented, and it is called the *Darboux frame*.

As $\bar{t}$, $\bar{n}$, $\bar{b}$ are differentiable and $|\bar{t}|^2_{I\!R^3} = |\bar{n}|^2_{I\!R^3} = |\bar{b}|^2_{I\!R^3} = 1 \quad \forall\, x_3 \in [0, L]$, it follows that

$$\langle \bar{t}, \bar{t}' \rangle = \langle \bar{n}, \bar{n}' \rangle = \langle \bar{b}, \bar{b}' \rangle = 0 \quad \text{in } [0, L]. \tag{2.7}$$

The orthogonality relations (2.7) give the "equations of motion" of the Darboux frame,

$$\begin{aligned} \bar{t}'(x_3) &= a(x_3)\,\bar{b}(x_3) + \beta(x_3)\,\bar{n}(x_3), \\ \bar{b}'(x_3) &= -a(x_3)\,\bar{t}(x_3) + c(x_3)\,\bar{n}(x_3), \\ \bar{n}'(x_3) &= -\beta(x_3)\,\bar{t}(x_3) - c(x_3)\,\bar{b}(x_3), \end{aligned} \tag{2.8}$$

where the functions $a(\cdot)$, $\beta(\cdot)$, $c(\cdot)$ are piecewise continuous and, in that order, are called the geodesic curvature, the normal curvature, and the geodesic torsion, respectively, of the curve $\bar{\theta}(\cdot)$, Cartan [4, p. 162].

The curved rod $\tilde{\Omega}$ is clamped at both ends, and it is subjected to body forces $\tilde{f}$ in $\tilde{\Omega}$ (weight, electromagnetic field, etc.) and to surface tractions $\tilde{g}$ on the lateral surface denoted $\tilde{\Sigma}$. Notice that, on the "inside" lateral face of $\tilde{\Omega}$ (i.e. corresponding to possible holes in the cross section), we have $\tilde{g} \equiv 0$.

We denote by $\bar{u} : \tilde{\Omega} \to I\!R^3$ the corresponding displacement of each point $\tilde{x} \in \tilde{\Omega}$ under the action of the given forces. Our "mechanical" assumption is that $\bar{u}$ has the form

$$\bar{u}(\tilde{x}) = \bar{\tau}(x_3) + x_1\,\bar{N}(x_3) + x_2\,\bar{B}(x_3) \quad \forall\, \tilde{x} \in \tilde{\Omega}, \tag{2.9}$$

with $\bar{x} = (x_1, x_2, x_3) = F^{-1}(\tilde{x})$ and where $\bar{\tau}$, $\bar{N}$, $\bar{B} \in H^1_0(0, L)^3$ are unknown functions.

Relation (2.9) is a special simple case of the so-called polynomial approximation of the displacement, used by Trabucho and Viaño [19], Delfour and Jiabin [11]. In particular, it says that transverse sections of $\tilde{\Omega}$ (i.e. perpendicular on $\bar{t}(x_3)$, $x_3 \in [0, L]$) remain plane or degenerate to dimension 1 after the deformation. The vector

$\bar\tau(x_3)$ describes the translation of the points on the centroid line $\bar\theta(\,\cdot\,)$, and the vectors $\bar N(x_3)+\bar n(x_3)$, $\bar B(x_3)+\bar b(x_3)$ show the deformation of the orthogonal frame in the cross section (which does not necessarily remain orthogonal to the tangent of the new centroid line, i.e. to $\bar\theta'(x_3)+\bar\tau'(x_3)$). This allows for shear and length or volume changes after the deformation.

By an obvious computation, we get the Jacobian of F, denoted by $J(\bar x)=DF(\bar x)$, its determinant, and its inverse (using (2.8)):

$$J(\bar x) \;=\; \begin{bmatrix} n_1(x_3) & b_1(x_3) & t_1(x_3) \,+\, x_1\, n_1'(x_3) \,+\, x_2\, b_1'(x_3) \\ n_2(x_3) & b_2(x_3) & t_2(x_3) \,+\, x_1\, n_2'(x_3) \,+\, x_2\, b_2'(x_3) \\ n_3(x_3) & b_3(x_3) & t_3(x_3) \,+\, x_1\, n_3'(x_3) \,+\, x_2\, b_3'(x_3) \end{bmatrix}, \tag{2.10}$$

$$J(\bar x)^{-1} = \begin{bmatrix} n_1 - \dfrac{c\,t_1\,x_2}{1-\beta\,x_1-a\,x_2} & n_2 - \dfrac{c\,t_2\,x_2}{1-\beta\,x_1-a\,x_2} & n_3 - \dfrac{c\,t_3\,x_2}{1-\beta\,x_1-a\,x_2} \\ b_1 + \dfrac{c\,t_1\,x_1}{1-\beta\,x_1-a\,x_2} & b_2 + \dfrac{c\,t_2\,x_1}{1-\beta\,x_1-a\,x_2} & b_3 + \dfrac{c\,t_3\,x_1}{1-\beta\,x_1-a\,x_2} \\ \dfrac{t_1}{1\,-\,\beta\,x_1-a\,x_2} & \dfrac{t_2}{1\,-\,\beta\,x_1-a\,x_2} & \dfrac{t_3}{1\,-\,\beta\,x_1-a\,x_2} \end{bmatrix}, \tag{2.11}$$

$$\det J(\bar x) \;=\; 1 \,-\, \beta(x_3)\,x_1 \,-\, a(x_3)\,x_2\,, \quad \forall\ \bar x \,\in\, \Omega\,. \tag{2.12}$$

If $\omega(x_3)$ is contained in a ball with a sufficiently small radius with respect to the curvatures, then we may assume that

$$\det J(\bar x) \;\geq\; c \,>\, 0\,, \quad \forall\ \bar x \,\in\, \Omega\,.$$

We introduce the vectorial mapping $\bar w : \Omega \to I\!R^3$,

$$\bar w(\bar x) \;=\; \bar\tau(x_3) \,+\, x_1\,\bar N(x_3) \,+\, x_2\,\bar B(x_3)\,, \quad \forall\ \bar x \,\in\, \Omega\,, \tag{2.13}$$

and we notice that

$$\bar u(\tilde x) \;=\; \bar w(F^{-1}\,(\tilde x))\ . \tag{2.14}$$

We recall that

$$D\,\bar u(\tilde x) = D\,\bar w(F^{-1}(\tilde x))\,D\,F^{-1}(\tilde x) = D\,\bar w(F^{-1}(\tilde x))\,J(F^{-1}(\tilde x))^{-1}\,,\ \forall\ \tilde x \,\in\, \tilde\Omega\,. \tag{2.15}$$

We simply denote:

$$D\,F^{-1}(\tilde x) \;=\; (d_{ij}(\tilde x))_{i,j=\overline{1,3}}\ ; \quad J(\bar x)^{-1} \;=\; (h_{ij}(\bar x))_{i,j=\overline{1,3}}\ . \tag{2.16}$$

By (2.10)–(2.16), we can compute the symmetrized gradients e_{ij} of the displacement $\bar u(\tilde x)$. We have

$$\begin{aligned} \frac{\partial u_i}{\partial \tilde x_j}(\tilde x) \;&=\; N_i(x_3(\tilde x))\,d_{1j}(\tilde x) \,+\, B_i(x_3(\tilde x))\,d_{2j}(\tilde x) \,+\, \Big[\tau_i'(x_3(\tilde x)) \\ &\quad + x_1(\tilde x)\,N_i'(x_3(\tilde x)) \,+\, x_2(\tilde x)\,B_i'(x_3(\tilde x))\Big]\,d_{3j}(\tilde x)\,, \quad i,j \,=\, \overline{1,3}\,; \end{aligned} \tag{2.17}$$

$$e_{ij}(\tilde{x}) \;=\; \frac{1}{2}\left(\frac{\partial u_i}{\partial \tilde{x}_j} \;+\; \frac{\partial u_j}{\partial \tilde{x}_i}\right)(\tilde{x})\,, \quad i,j \;=\; \overline{1,3}\,. \tag{2.18}$$

Consequently, we get (without summation convention)

$$e_{ii}(\tilde{x}) \;=\; \frac{\partial u_i}{\partial \tilde{x}_i}\,(\tilde{x})\,, \quad i \;=\; \overline{1,3}\,, \tag{2.19}$$

$$\begin{aligned} e_{ij}(\tilde{x}) \;=\; e_{ji}(\tilde{x}) \;=\; \tfrac{1}{2}\Big\{ & N_i(x_3(\tilde{x}))\, d_{1j}(\tilde{x}) \;+\; B_i(x_3(\tilde{x}))\, d_{2j}(\tilde{x}) \\ & + \Big[\tau_i'(x_3(\tilde{x})) \;+\; x_1(\tilde{x})\, N_i'(x_3(\tilde{x})) \;+\; x_2(\tilde{x})\, B_i'(x_3(\tilde{x}))\Big]\, d_{3j}(\tilde{x}) \\ & + N_j(x_3(\tilde{x}))\; d_{1i}(\tilde{x}) + \; B_j(x_3(\tilde{x}))\; d_{2i}(\tilde{x}) \;+\; \Big[\tau_j'(x_3(\tilde{x})) \\ & + x_1(\tilde{x})\, N_j'(x_3(\tilde{x})) \;+\; x_2(\tilde{x})\, B_j'(x_3(\tilde{x}))\Big]\, d_{3i}(\tilde{x})\Big\}\,, \quad i,j \;=\; \overline{1,3}\,. \end{aligned} \tag{2.20}$$

If $\lambda, \mu > 0$ denote the Lamé constants of the material, the bilinear form governing the equations of linear elasticity is defined on the subspace $\tilde{Z}\times\tilde{Z} \subset H^1(\tilde{\Omega})^3 \times H^1(\tilde{\Omega})^3$ of functions having zero traces on the "bases" of the rod $\tilde{\Omega}$, i.e. on $F(\omega(0)) \cup F(\omega(L))$. We have (with summation convention):

$$\mathcal{B}(\bar{u},\bar{v}) \;=\; \int\limits_{\tilde{\Omega}} \Big[\lambda\, e_{pp}(\bar{u})\, e_{qq}(\bar{v}) \;+\; 2\mu\, e_{ij}(\bar{u})\, e_{ij}(\bar{v})\Big]\, d\tilde{x}\,. \tag{2.21}$$

Notice that $\bar{u}$ given by (2.9) belongs to $\tilde{Z}$, and we shall take the test functions $\bar{v} \in \tilde{Z}$ in a similar form by replacing the unknown mappings N_i, B_i, τ_i, respectively, by some arbitrary mappings M_i, D_i, $\mu_i \in H_0^1(0,L)$, $i = \overline{1,3}$. In this way, we perform a projection of $\mathcal{B}$ onto the (infinite dimensional) subspace $Z \subset \tilde{Z}$ of all mappings $\bar{u}$ given by (2.9) with "coefficients" $\bar{\tau}, \bar{N}, \bar{B} \in H_0^1(0,L)^3$. We underline that this is essentially the same procedure as in the finite element method (where finite dimensional subspaces appear), and some convergence and approximation results are proved by Trabucho and Viaño [19] in a different setting. By the above choice, it is obvious that the space Z can be identified with $H_0^1(0,L)^9$. A standard change of variables, and (2.9), (2.16), give

$$\begin{aligned} \mathcal{B}(\bar{u},\bar{v}) \;=\; & \int\limits_{F(\Omega)} \Big[\lambda\, e_{pp}(\bar{u})\,(F\bar{x}) \;\cdot\; e_{qq}(\bar{v})\,(F\bar{x}) \;+\; 2\mu\, e_{ij}(\bar{u})\,(F\bar{x}) \;\cdot\; e_{ij}(\bar{u})(F\bar{x})\Big]\, d\tilde{x} \\ = \lambda \int\limits_{\Omega} & \sum_{i,j=1}^{3} \Big[N_i(x_3) h_{1i}(\bar{x}) + B_i(x_3)\, h_{2i}(\bar{x}) + \Big(\tau_i'(x_3) + x_1 N_i'(x_3) + x_2 B_i'(x_3)\Big) h_{3i}(\bar{x})\Big] \\ & \times \Big[M_j(x_3)\, h_{1j}(\bar{x}) \;+\; D_j(x_3)\, h_{2j}(\bar{x}) \;+\; \Big(\mu_j'(x_3) \;+\; x_1\, M_j'(x_3) \;+\; x_2\, D_j'(x_3)\Big)\, h_{3j}(\bar{x})\Big] \\ & \times \Big|\det J(\bar{x})\Big|\, d\bar{x} \;+\; \mu \int\limits_{\Omega} \sum_{i\neq j} \Big[N_i(x_3)\, h_{1j}(\bar{x}) \;+\; B_i(x_3)\, h_{2j}(\bar{x}) \;+\; \Big(\tau_i'(x_3) + x_1\, N_i'(x_3) \\ & + x_2\, B_i'(x_3)\Big)\, h_{3j}(\bar{x}) \;+\; N_j(x_3)\, h_{1i}(\bar{x}) \;+\; B_j(x_3)\, h_{2i}(\bar{x}) \;+\; \Big(\tau_j'(x_3) \;+\; x_1\, N_j'(x_3) + \end{aligned}$$

$$+ x_2\, B_j'(x_3)\Big)\, h_{3i}(\bar{x})\Big]\Big[M_i(x_3)\, h_{1j}(\bar{x}) \,+\, D_i(x_3)\, h_{2j}(\bar{x}) \,+\, \Big(\mu_i'(x_3) \,+\, x_1\, M_i'(x_3)$$
$$+ x_2\, D_i'(x_3)\Big)\, h_{3j}(\bar{x}) \,+\, M_j(x_3)\, h_{1i}(\bar{x}) \,+\, D_j(x_3)\, h_{2i}(\bar{x}) \,+\, \Big(\mu_j'(x_3) \,+\, x_1\, M_j'(x_3)$$
$$+ x_2 D_j'(x_3)\Big)\, h_{3i}(\bar{x})\Big]\Big|\det J(\bar{x})\Big|\, d\bar{x} \,+\, 2\mu \int\limits_{\Omega} \sum_{i=1}^{3} \Big[N_i(x_3)\, h_{1i}(\bar{x}) \,+\, B_i(x_3)\, h_{2i}(\bar{x})$$
$$+ \Big(\tau_i'(x_3) \,+\, x_1\, N_i'(x_3) \,+\, x_2\, B_i'(x_3)\Big)\, h_{3i}(\bar{x})\Big]\Big[M_i(x_3)\, h_{1i}(\bar{x}) \,+\, D_i(x_3)\, h_{2i}(\bar{x})$$
$$+ \Big(\mu_i'(x_3) \,+\, x_1\, M_i'(x_3) \,+\, x_2\, D_i'(x_3)\Big)\, h_{3i}(\bar{x})\Big]\Big|\det J(\bar{x})\Big|\, d\bar{x}\,. \qquad (2.22)$$

We have the following result.

Theorem 2.1 *Assume that* $0 < C \le 1 - \beta(x_3)\, x_1 - a(x_3)\, x_2 \le m$, $\forall\, \bar{x} \in \Omega$. *Then, the bilinear form* $\mathcal{B}$ *is coercive and bounded on* $H_0^1(0,L)^9$.

The argument follows the same steps as in the proof given by Ciarlet [9] for the case of plane arches.

We start with the following new inequality:

Lemma 2.2 *There are* $c_1 > 0$, $c_2 > 0$ *such that*

$$\mathcal{B}(\bar{u},\bar{u}) \,\ge\, c_1 \Big|\bar{u}\Big|^2_{H_0^1(0,L)^9} \,-\, c_2 \Big|\bar{u}\Big|^2_{L^2(0,L)^9}\,, \qquad (2.23)$$

where $\bar{u}$, *given by* (2.9), *is identified with the vector* $(\tau_1\,,\,\tau_2\,,\,\tau_3\,,\,N_1\,,\,N_2\,,\,N_3\,,\,B_1\,,\,B_2,\, B_3) \in H_0^1(0,L)^9$.

Proof. By virtue of (2.22), (2.12), and since $\omega(x_3) \supset \omega$, $\forall\, x_3 \in [0,L]$, we have

$$\mathcal{B}(\bar{u},\bar{u}) \,\ge\, \mu\, c \int\limits_{\omega\times[0,L]} \sum_{i\neq j} \Big[N_i(x_3)\, h_{1j}(\bar{x}) \,+\, B_i(x_3)\, h_{2j}(\bar{x}) \,+\, \Big(\tau_i'(x_3) \,+\, x_1\, N_i'(x_3)$$
$$+ x_2\, B_i'(x_3)\Big)\, h_{3j}(\bar{x}) \,+\, N_j(x_3)\, h_{1i}(\bar{x}) \,+\, B_j(x_3)\, h_{2i}(\bar{x}) \,+\, \Big(\tau_j'(x_3) \,+\, x_1\, N_j'(x_3)$$
$$+ x_2\, B_j'(x_3)\Big)\, h_{3i}(\bar{x})\Big]^2\, d\bar{x} \,+\, 2\mu\, c \int\limits_{\omega\times[0,L]} \sum_{i=1}^{3} \Big[N_i(x_3)\, h_{1i}(\bar{x}) \,+\, B_i(x_3)\, h_{2i}(\bar{x})$$
$$+ \Big(\tau_i'(x_3) \,+\, x_1\, N_i'(x_3) \,+\, x_2\, B_i'(x_3)\Big)\, h_{3i}(\bar{x})\Big]^2\, d\bar{x}\,.$$

Consequently, usual binomial inequalities imply that

$$\frac{1}{\mu\, c}\mathcal{B}(\bar{u},\bar{u}) \,\ge\, \frac{1}{2} \int\limits_{\omega\times[0,L]} \sum_{i\neq j} \Big[\Big(\tau_i'(x_3) \,+\, x_1\, N_i'(x_3) \,+\, x_2\, B_i'(x_3)\Big)\, h_{3j}(\bar{x})$$
$$+ \Big(\tau_j'(x_3) \,+\, x_1\, N_j'(x_3) \,+\, x_2\, B_j'(x_3)\Big)\, h_{3i}(\bar{x})\Big]^2 \,+\, \int\limits_{\omega\times[0,L]} \sum_{i=1}^{3} \Big[\Big(\tau_i'(x_3) \,+\, x_1\, N_i'(x_3)$$
$$+ x_2\, B_i'(x_3)\Big)\, h_{3i}(\bar{x})\Big]^2\, d\bar{x} \,-\, C|\bar{u}|^2_{L^2(0,L)^9}\,, \qquad (2.24)$$

where we have used that $h_{ij} \in L^\infty(\Omega)$, $i,j = \overline{1,3}$, which follows from (2.10)–(2.12), (2.16), and from the regularity of the curve $\bar\theta(\,\cdot\,)$ and of the Darboux frame.

We denote, for simplicity, $z_i = \tau_i' + x_1 N_i' + x_2 B_i'$, $i = \overline{1,3}$.

We make an algebraic computation:

$$\begin{aligned}
&\frac{1}{2}\Big[(z_1\,h_{32} \,+\, z_2\,h_{31})^2 \,+\, (z_2\,h_{33} \,+\, z_3\,h_{32})^2 \,+\, (z_1\,h_{33} \,+\, z_3\,h_{31})^2\Big] \\
&+\frac{3}{2}(z_1^2\,h_{31}^2 \,+\, z_2^2\,h_{32}^2 \,+\, z_3^2\,h_{33}^2) \\
=\;& \frac{1}{2}z_1^2\,h_{32}^2 \,+\, \frac{1}{2}z_2^2\,h_{31}^2 \,+\, \frac{1}{2}z_2^2\,h_{33}^2 \,+\, \frac{1}{2}z_3^2\,h_{32}^2 \,+\, \frac{1}{2}z_1^2\,h_{33}^2 \,+\, \frac{1}{2}z_3^2\,h_{31}^2 \,+ z_1\,z_2\,h_{31}\,h_{32} \\
&+ z_2\,z_3\,h_{32}\,h_{33} \,+\, z_1\,z_3\,h_{31}\,h_{33} \,+\, \frac{3}{2}(z_1^2\,h_{31}^2 \,+\, z_2^2\,h_{32}^2 \,+\, z_3^2\,h_{33}^2) \\
=\;& \frac{1}{2}(z_1^2 \,+\, z_2^2 \,+\, z_3^2)(h_{31}^2 \,+\, h_{32}^2 \,+\, h_{33}^2) \,+\, \frac{1}{2}(z_1\,h_{31} \,+\, z_2\,h_{32})^2 \\
&+\frac{1}{2}(z_1\,h_{31} \,+\, z_3\,h_{33})^2 \,+\, \frac{1}{2}(z_2\,h_{32} \,+\, z_3\,h_{33})^2\,.
\end{aligned}$$

Hence, we can infer from (2.24) that

$$\begin{aligned}
\frac{1}{c\,\mu}\mathcal{B}(\bar u,\bar u) \;\ge\; \frac{1}{4}\int\limits_{\omega\times[0,L]} \sum_{i=1}^{3} \Big(\tau_i'(x_3) \,+\, x_1\,N_i'(x_3) \\
+\, x_2\,B_i'(x_3)\Big)^2 \sum_{i=1}^{3} h_{3i}^2(\bar x)\,d\bar x \;-\; C|\bar u|^2_{L^2(0,L)^9}\,. \qquad (2.25)
\end{aligned}$$

Examining (2.11), we see that, under the assumption of the theorem,

$$\begin{aligned}
\sum_{i=1}^{3} h_{3i}^2 \;&=\; \frac{1}{(1-\beta(x_3)\,x_1 - a(x_3)\,x_2)^2}\sum_{i=1}^{3} t_i(x_3)^2 = \frac{1}{(1-\beta(x_3)\,x_1 - a(x_3)\,x_2)^2} \\
&\ge\; \kappa \,>\, 0 \qquad (2.26)
\end{aligned}$$

for some $\kappa > 0$, since $|\bar t|_{I\!R^3} = 1$.

Let us also note that, owing to (2.1), we have

$$\begin{aligned}
&\int\limits_{\omega\times[0,L]} \Big(\tau_i'(x_3) \,+\, x_1\,N_i'\,(x_3) \,+\, x_2\,B_i'(x_3)\Big)^2\,d\bar x \\
=\;& \mathrm{meas}(\omega)|\tau_i|^2_{H_0^1(0,L)} \,+\, \int\limits_{\omega} x_1^2\,dx_1\,dx_2\,|N_i|^2_{H_0^1(0,L)} \,+\, \int\limits_{\omega} x_2^2\,dx_1\,dx_2\,|B_i|^2_{H_0^1(0,L)}\,, \\
&i \,=\, \overline{1,3}\,, \qquad (2.27)
\end{aligned}$$

with $\mathrm{meas}(\omega)$ denoting the Lebesgue measure in $I\!R^2$ of the domain ω.

By combining (2.25)–(2.27), we end the proof. □

Lemma 2.3 *If* $\mathcal{B}(\bar{u},\bar{u}) = 0$, *then* $\bar{u} = 0$.

Proof. If $B(\bar{u},\bar{u}) = 0$, we obtain for a.e. $\bar{x} \in \Omega$ that

$$N_i(x_3)\, h_{1i}(\bar{x}) \,+\, B_i(x_3)\, h_{2i}(\bar{x}) \,+\, z_i\, h_{3i}(\bar{x}) \,=\, 0\,, \quad \forall\ i \,=\, \overline{1,3}\,, \tag{2.28}$$

$$\begin{aligned} N_i(x_3)\, h_{1j}(\bar{x}) \,+ B_i(x_3)\, h_{2j}(\bar{x}) \,+\, N_j(x_3)\, h_{1i}(\bar{x}) \,+\, B_j(x_3)\, h_{2i}(\bar{x}) \\ + z_i\, h_{3j}(\bar{x}) \,+\, z_j\, h_{3i}(\bar{x}) \,=\, 0\,, \quad i \,\neq\, j\,, \quad i,j \,=\, \overline{1,3}\,, \end{aligned} \tag{2.29}$$

with z_i as in the previous proof.

Multiply (2.29) by $h_{3i}(\bar{x})$ and (2.28) by $h_{3j}(\bar{x})$ (j is fixed!) and subtract. Then multiply (2.28) by $h_{3i}(\bar{x})$ for $i = j$, and add to the previous results, obtained for $i \neq j$. We get:

$$\tilde{\Gamma}(\bar{N},\bar{B}) \,+\, z_j \sum_{i=1}^{3} h_{3i}^2(\bar{x}) \,=\, 0\,, \quad \forall\ j \,=\, \overline{1,3}\,, \tag{2.30}$$

with $\tilde{\Gamma}(\bar{N},\bar{B})$ some linear mapping of the vectors $\bar{N},\bar{B}$. Taking into account (2.11) and $|\bar{t}|_{I\!R^3} = 1$, (2.30) gives:

$$\tau_i'(x_3) \,+\, x_1\, N_i'(x_3) \,+\, x_2\, B_i'(x_3) \,=\, \Gamma(\bar{N},\bar{B})\,, \quad \forall\ i \,=\, \overline{1,3}\,, \tag{2.31}$$

with Γ a clear modification of $\tilde{\Gamma}$.

For any i , we give to $(x_1,x_2) \in \omega$ three different pairs of values, and we obtain a linear differential system in normalized form with zero initial conditions, since τ_i , N_i , $B_i \in H_0^1(0,L)$, $\forall i = \overline{1,3}$. Then, the unique solution is identically zero and this gives that $\bar{u} = 0$ in Ω as claimed. Here, we have again used that the coefficients h_{ij} are bounded. □

Proof of Theorem 2.1. Assume, by contradiction, that for any $\varepsilon > 0$ there is $u_\varepsilon = (\tau_1^\varepsilon\,,\, \tau_2^\varepsilon\,,\, \tau_3^\varepsilon\,,\, N_1^\varepsilon\,,\, N_2^\varepsilon\,,\, N_3^\varepsilon\,,\, B_1^\varepsilon\,,\, B_2^\varepsilon\,,\, B_3^\varepsilon) \in H_0^1(0,L)^9$ such that

$$0 \,\leq\, \mathcal{B}(u_\varepsilon,u_\varepsilon) \,\leq\, \varepsilon |u_\varepsilon|^2_{H_0^1(0,L)^9}\,.$$

Without loss of generality, we may take $|u_\varepsilon|_{H_0^1(0,L)^9} = 1$, and we denote by $\hat{u}$ the weak limit in $H_0^1(0,L)^9$, on a subsequence of $\{u_\varepsilon\}$.

The weak lower semicontinuity of the quadratic form gives

$$0 \,\leq\, \mathcal{B}(\hat{u},\hat{u}) \,\leq\, 0\,,$$

i.e. $B(\hat{u},\hat{u}) = 0$ and $\hat{u} = 0$ by **Lemma 2.3**.

We get that $u_\varepsilon \to 0$ weakly in $H_0^1(0,L)^9$ and, by compact imbedding, strongly in $L^2(0,L)^9$. We use **Lemma 2.2** for u_ε , and we pass to the limit in the inequality (2.23) to obtain that

$$\varepsilon \,\geq\, B(u_\varepsilon,u_\varepsilon) \,\geq\, c_1 |u_\varepsilon|^2_{H_0^1(0,L)^9} \,-\, c_2 |u_\varepsilon|^2_{L^2(0,L)^9} \,=\, c_1 \,-\, c_2 |u_\varepsilon|^2_{L^2(0,L)^9}\,.$$

Consequently, we obtain the contradiction

$$0 \ \geq \ c_1 \, ,$$

which ends the proof of **Theorem 2.1**. □

According to the linear elasticity system and to our assumptions, the displacement $\bar{u}$, defined by (2.9), is obtained as the solution of the variational equation:

$$\mathcal{B}(\bar{u}, \bar{v}) \ = \ \int\limits_{\Omega} f_\ell(\bar{x}) \Big(\mu_\ell(x_3) \ + \ x_1 \, M_\ell(x_3) \ + \ x_2 \, D_\ell(x_3) \Big) \ \Big| \det J(\bar{x}) \Big| \, d\bar{x}$$

$$+ \int\limits_{\partial\Omega} g_\ell(\bar{x}) \Big(\mu_\ell(x_3) + x_1 \, M_\ell(x_3) + x_2 \, D_\ell(x_3) \Big) \ \Big| \det J(\bar{x}) \Big| \ \sqrt{\nu_i(\bar{x}) \, g^{ij}(\bar{x}) \, \nu_j(\bar{x})} \, d\tau, \quad (2.32)$$

where (ν_i) is the unit outside normal to $\partial\Omega$ and the summation convention is used.

We recall that $(\tilde{f}_i)_{i=\overline{1,3}}$ and $(\tilde{g}_i)_{i=\overline{1,3}}$ are the body forces, respectively the surface tractions, acting on the curved rod $\tilde{\Omega}$, and we have denoted by $\bar{f} = (f_\ell)_{\ell=\overline{1,3}}$ and $\bar{g} = (g_\ell)_{\ell=\overline{1,3}}$ the quantities:

$$\bar{f}(\bar{x}) \ = \ \tilde{f}(F \, \bar{x}) \, , \quad \bar{g}(\bar{x}) \ = \ \tilde{g}(F \, \bar{x}) \, . \quad (2.33)$$

The coefficients $g^{ij}(\bar{x})$ are obtained as (Ciarlet [10])

$$\Big(g_{ij}(\bar{x}) \Big)_{i,j=\overline{1,3}} \ = \ J(\bar{x})^T \, J(\bar{x}) \, , \quad (2.34)$$

$$\Big(g^{ij}(\bar{x}) \Big)_{i,j=\overline{1,3}} \ = \ \Big(g_{ij}(\bar{x}) \Big)^{-1}_{i,j=\overline{1,3}} . \quad (2.35)$$

The right-hand side in (2.32), and the relations (2.33)–(2.35), are due to a standard change of variable $\tilde{\Omega} \mapsto \Omega$ in the integrals

$$\int\limits_{\tilde{\Omega}} \tilde{f}_i \, \tilde{v}_i \, d\tilde{x} \ + \ \int\limits_{\tilde{\Sigma}} \tilde{g}_i \, \tilde{v}_i \, d\tilde{\tau} \, , \quad (\tilde{v}_i)_{i=\overline{1,3}} \ \in \ H^1(\tilde{\Omega})^3 \, , \tilde{v}_i \ = \ 0 \ \text{on} \ F\Big(\omega(0) \ \cup \ \omega(L) \Big) \, ,$$

which express the action on the rod $\tilde{\Omega}$.

It should be noted that at least Lipschitz regularity is necessary for the part of $\partial\Omega$ where the tractions are nonzero, which represents a hypothesis on the "variation" of the cross sections $\omega(x_3)$. If ω is constant and $\partial\omega$ is smooth, then (2.32) is fully justified.

Corollary 2.4 *Under the above assumptions, equation* (2.32) *has a unique solution in* $H^1_0(0, L)^9$.

3 A direct approach

In this section, we study general rods associated with the three-dimensional curve $\bar{\theta} : [0, L] \to I\!R^3$, $\bar{\theta} \in W^{2,\infty}(0, L)^3$, with $\bar{\theta}''$ piecewise continuous, parametrized with respect to the arc length which are no more assumed to lie on some given surface. In this setting, it is possible to define the Frenet frame with normal and binormal vectors in $L^\infty(0, L)^3$. However, this property is not enough for the study of the corresponding geometric transformation defining the rod and of the associated differential equations, and that is why the standard assumption in the literature is $\bar{\theta} \in C^3[0, L]^3$.

We define a new Lipschitzian local frame, simple to use in numerical computations, and requiring just $\bar{\theta} \in W^{2,\infty}(0, L)^3$. Our construction also applies to curves from $C^1[0, L]^3$, but in this case the local basis vectors are in $C[0, L]^3$. In particular, we notice that all the vectors of this basis have the same regularity as the tangent vector.

For any $s \in [0, L]$, we define as in Section 2, $\bar{t}(s) = \bar{\theta}'(s)$, the unit tangent vector to $\bar{\theta}$, and $\bar{t} \in W^{1,\infty}(0, L)^3$.

Let $\{s_i\}$, $i = \overline{0, N+1}$, be a partition of the interval $[0, L]$ with $s_0 = 0$ and $s_{N+1} = L$, and with a sufficiently small norm in the sense that

$$\left|\bar{t}(s_i) - \bar{t}(s_{i+1})\right|_{I\!R^3} < \delta\,, \quad \forall\, i = \overline{0, N}\,, \tag{3.1}$$

with $\delta > 0$ "small". This can be obtained due to the assumed uniform continuity of $\bar{t}(\,\cdot\,)$ in $[0, L]$.

For $i = \overline{0, N+1}$, we define the vectors

$$\tilde{n}(s_i) = \begin{cases} \Big(0, -\theta_3'(s_i), \theta_2'(s_i)\Big) \Big/ \sqrt{\theta_3'(s_i)^2 + \theta_2'(s_i)^2} & \text{if } \Big(\theta_2'(s_i), \theta_3'(s_i)\Big) \neq (0,0)\,, \\ \Big(0, \theta_1'(s_i), 0\Big) \Big/ \Big|\theta_1'(s_i)\Big| & \text{otherwise}\,. \end{cases} \tag{3.2}$$

We have:

$$\left|\tilde{n}(s_i)\right|_{I\!R^3} = 1\,, \quad \tilde{n}(s_i) \perp \bar{t}(s_i)\,, \quad i = \overline{0, N+1}\,. \tag{3.3}$$

We can also assume that the angle between $\tilde{n}(s_i)$, $\tilde{n}(s_{i+1})$ is acute, i.e. that

$$\langle \tilde{n}(s_i)\,, \tilde{n}(s_{i+1}) \rangle \geq 0\,, \quad i = \overline{0, N}\,. \tag{3.4}$$

This can simply be achieved by changing $\tilde{n}(s_{i+1})$ into $-\tilde{n}(s_{i+1})$, if necessary, and iterating the process from s_1 to s_{N+1}. We denote by $\bar{n}(s_i)$ the thus obtained vectors.

On each interval $[s_i, s_{i+1}]$, we build the function

$$\bar{m}_i(s) = \bar{n}(s_i) + \frac{s - s_i}{s_{i+1} - s_i}\Big[\bar{n}(s_{i+1}) - \bar{n}(s_i)\Big]\,, \quad i = \overline{0, N}\,. \tag{3.5}$$

Clearly, $\bar{m}_i(s_i) = \bar{n}_i(s_i)$, $\bar{m}_i(s_{i+1}) = \bar{n}_i(s_{i+1})$, and the function $\bar{m}(s) = \bar{m}_i(s)$, $s \in [s_i, s_{i+1}]$, is Lipschitz in $[0, L]$. Moreover, we have

$$\left|\bar{m}_i(s)\right|_{I\!R^3} \geq \frac{\sqrt{2}}{2}, \quad \forall\, s \in [0, L], \quad \forall\, i = \overline{0, N}. \tag{3.6}$$

Inequality (3.6) is a consequence of elementary geometric arguments in the triangle with two unit edges $\bar{n}(s_i)$, $\bar{n}(s_{i+1})$ and with an acute angle, using (3.4). We just notice that $|\bar{m}_i(s_i)|_{I\!R^3}$ is the length of the line segment connecting arbitrary points on the "basis" of this triangle with its "top" point, whence (3.6) easily follows.

Assume, for the moment, that $\bar{m}(\hat{s})$ is collinear with $\bar{t}(\hat{s})$, for some $\hat{s} \in [0, L]$. Since $|\bar{t}(\hat{s})|_{I\!R^3} = 1$, we get from (3.5) that

$$\bar{n}(s_i) + \frac{\hat{s} - s_i}{s_{i+1} - s_i}\Big[\bar{n}(s_{i+1}) - \bar{n}(s_i)\Big] = \pm\left|\bar{m}_i(\hat{s})\right|_{I\!R^3}\bar{t}(\hat{s}), \tag{3.7}$$

where i is fixed such that $\hat{s} \in [s_i, s_{i+1}]$. We multiply (3.7) by $\bar{t}(\hat{s})$ and apply (3.6), the triangle inequality, and the Cauchy–Schwarz inequality, to obtain that

$$\begin{aligned}\frac{\sqrt{2}}{2} \;\leq\; \left|\bar{m}_i(\hat{s})\right|_{I\!R^3} &\leq \left(1 - \frac{\hat{s} - s_i}{s_{i+1} - s_i}\right)\left|\bar{t}(\hat{s}) - \bar{t}(s_i)\right|_{I\!R^3} \\ &+ \frac{\hat{s} - s_i}{s_{i+1} - s_i}\left|\bar{t}(\hat{s}) - \bar{t}(s_{i+1})\right|_{I\!R^3} \leq \delta. \end{aligned} \tag{3.8}$$

Here, we have also used (3.1) and (3.3).

As (3.8) is a contradiction for δ "small", we infer that $\bar{m}(s)$ and $\bar{t}(s)$ are linearly independent vectors for any $s \in [0, L]$. We thus can apply the Schmidt orthogonalization process to them and construct:

$$\tilde{n}(s) = \bar{m}(s) - \Big\langle \bar{m}(s), \bar{t}(s) \Big\rangle\, \bar{t}(s), \tag{3.9}$$

$$\bar{n}(s) = \tilde{n}(s) \Big/ |\tilde{n}(s)|_{I\!R^3}, \quad s \in [0, L]. \tag{3.10}$$

Notice that $\tilde{n}(s) \neq (0, 0, 0)$ due to the linear independence and, moreover, $|\tilde{n}(s)|_{I\!R^3} \geq$ constant > 0 due to its continuity.

This shows that $\bar{n}(s)$ as defined by (3.9), (3.10) has the same smoothness as $\bar{t}(s)$ since $\bar{m}(s)$ is Lipschitzian. We have proved:

Theorem 3.1 *If $\bar{\theta} \in C^1[0, L]^3$ $(W^{2,\infty}(0, L)^3)$ then $\bar{n} \in C[0, L]^3$ $(W^{1,\infty}(0, L)^3)$, and $|\bar{n}(s)|_{I\!R^3} = 1$, $\langle \bar{n}(s), \bar{t}(s)\rangle = 0$, $s \in [0, L]$. The vector function $\bar{b} = \bar{t} \wedge \bar{n}$ has the same regularity properties and completes the local frame.*

Remark. There are alternative ideas for the construction of normal vectors $\bar{n}$. For instance, starting with a smooth regularization $\bar{\theta}_\varepsilon$ of $\bar{\theta}$, to use the Frenet frame for $\bar{\theta}_\varepsilon$ and the Schmidt orthogonalization for the pair $\bar{t}$, $\bar{n}_\varepsilon$, with $\bar{n}_\varepsilon$ the normal

corresponding to $\bar{\theta}_\varepsilon$. However, the procedure given in **Theorem 3.1** seems to be more appropriate for numerical implementation.

Remark. In the case $\bar{\theta} \in C^1[0,L]^3$, **Theorem 3.1** provides a nondifferentiable local frame, which is not sufficient for the geometrical description and the solution of the differential equations associated to curved rods. However, it is simple to see that, even for rods with "corners" (for instance a rectangular thin frame of metal), one can provide a description of $\tilde{\Omega}$ as in (2.2)–(2.4) with $\bar{\theta}$ smooth, since we allow the cross sections $\omega(\,\cdot\,)$ to be nonconstant — see (2.1). Taking into account the difficulty of the asymptotic theory for curved rods, Trabucho and Viaño [15, § 38], when the thickness of the rod tends to zero, the reparametrization of a rod with corners via smooth $\bar{\theta}$ may become very complicated, or hypothesis (2.1) may be violated, etc. We shall analyze this question in a subsequent work.

Remark. With the local basis provided by **Theorem 3.1**, the same arguments as in Section 2 work for proving the coercivity, and the deformation of the curved rod is computed in a similar way. It is only here that the piecewise continuity of $\bar{\theta}''$ is necessary.

4 Numerical examples

We have tested both modelling approaches indicated in this paper on a large class of examples involving various geometrical shapes for the line of centroids, various cross sections and several types of applied forces.

As three-dimensional curves, we have considered the spiral

$$\bar{\theta}(t) \,=\, \left(\cos\frac{t}{\sqrt{2}}\,,\,\sin\frac{t}{\sqrt{2}}\,,\,\frac{t}{\sqrt{2}}\right)\,, \tag{4.1}$$

lying on the cylinder $x_1^2 + x_2^2 = 1$ and clamped at the endpoints,

$$T_1 \,=\, -\,\frac{\pi}{\sqrt{2}}\,,\quad T_2 \,=\, \frac{\pi}{\sqrt{2}}\,, \tag{4.2}$$

$$T_1 \,=\, 0\,,\quad T_2 \,=\, 8\,\pi\,\sqrt{2}\,. \tag{4.3}$$

The example (4.1), (4.2) was also discussed by Arunakirinathar and Reddy [3], and by Chapelle [7], by using the Frenet frame, while our method is based on the Darboux frame, as explained in Section 2.

Another form of the line of centroids (a "decreasing" spiral) is given by

$$\bar{\theta}(t) \,=\, \left(-\,\frac{(6\pi\,-\,t)^2}{20}\cos t\,,\,-\,\frac{(6\pi\,-\,t)^2}{20}\sin t\,,\,t\right)\,,\quad t\,\in\,[0,4\pi]\,, \tag{4.4}$$

which is inspired by the modern access to the new dome-shaped cupola of the Reichstag in Berlin. In this case, we have tested the direct geometrical approach

from Section 3, although it is clearly possible to define a surface (a paraboloid) including $\bar{\theta}$ as given by (4.4). Notice, as well, that the parametrization (4.4) is not with respect to the arc length, and the standard reparametrization is given by $s(0) = 0$, $s' = |\bar{\theta}'|_{I\!R^3}$, $\bar{\theta}_1(t) = \bar{\theta}(s^{-1}(t))$. While this relation is difficult to integrate, in general, we remark that in the direct approach of Section 3, just $\bar{\theta}_1' = \bar{\theta}'/|\bar{\theta}|_{I\!R^3}$ is needed, which is very easy to obtain.

Our choice of cross sections includes:

a) – disk of radius 0.3 centered in the points of $\bar{\theta}(\,\cdot\,)$:

$$x_1^2 + x_2^2 \leq 0.3^2 ;$$

b) – elliptical crown, centered in the points of $\bar{\theta}(\,\cdot\,)$

$$0.3^2 \leq \frac{{x_1}^2}{1} + \frac{{x_2}^2}{16} \leq 0.5^2 ;$$

c) – rectangle with dimension 0.6×0.2 centered in the points of $\bar{\theta}(\,\cdot\,)$.

The curved rods described above were "subjected" to distributed forces of the following types:

– torsional force

$$f(x_1, x_2, x_3) = (-x_2, x_1, 0)\,, \quad x_3 \in \left[-\frac{\pi}{\sqrt{2}}\,, \frac{\pi}{\sqrt{2}}\right] ; \tag{4.5}$$

– torsional force in two opposite directions

$$f(x_1, x_2, x_3) = \begin{cases} (-x_2, x_1, 0)\,, & x_3 \in \left[-\dfrac{\pi}{\sqrt{2}}\,, 0\right], \\ (x_2, -x_1, 0)\,, & x_3 \in \left[0, \dfrac{\pi}{\sqrt{2}}\right] ; \end{cases} \tag{4.6}$$

– pushing in one or two opposite given directions

$$f(x_1, x_2, x_3) = (0, 0, 1)\,, \quad x_3 \in \left[-\frac{\pi}{\sqrt{2}}\,, \frac{\pi}{\sqrt{2}}\right] , \tag{4.7}$$

$$f(x_1, x_2, x_3) = \begin{cases} (0, 0, 1) & x_3 \in \left[T_1, \dfrac{T_1 + T_2}{2}\right] , \\ (0, 0, -1) & x_3 \in \left[\dfrac{T_1 + T_2}{2}, T_2\right] , \end{cases} \tag{4.8}$$

$$f(x_1, x_2, x_3) = \begin{cases} (0, 0, -1000)\,, & x_3 \in [2\pi, 3\pi], \\ (0, 0, 0) & \text{otherwise} ; \end{cases} \tag{4.9}$$

– tangential forces

$$f(x_1, x_2, x_3) = \begin{cases} \bar{\theta}'(x_3)\,, & x_3 \in \left[T_1, \dfrac{T_1 + T_2}{2}\right] , \\ -\bar{\theta}'(x_3)\,, & x_3 \in \left[\dfrac{T_1 + T_2}{2}, T_2\right] , \end{cases} \tag{4.10}$$

– normal forces

$$f(x_1, x_2, x_3) = \bar{n}(x_3)\,, \tag{4.11}$$

where $\bar{n}(\cdot)$ is computed from the Darboux frame, i.e. is given by the normal to the cylinder containing $\bar{\theta}(\cdot)$, in the points of the curve $\bar{\theta}(\cdot)$. We also mention that, in all cases where the Darboux frame was applied, the computation of $\bar{t}$, $\bar{n}$, $\bar{b}$ and of the quantities $\det J(\bar{x})$, $h_{ij}(\bar{x})$, $a(x_3)$, $\beta(x_3)$, $c(x_3)$ was performed exactly, by using Mathematica. The same holds for all the graphical representations. For the method developed in Section 3, direct numerical calculations have been done to obtain the above parameters in the discretization points.

In Table 1, we have collected details about the geometrical and mechanical data assumed in the examples:

Table 1

Example	**Interval**	**Force**	**Section**	**Curve**	**Scaling**
1	(4.2)	(4.5)	a)	(4.1)	50
2	(4.2)	(4.6)	a)	(4.1)	500
3	(4.3)	(4.8)	a)	(4.1)	0.2
4	(4.2)	(4.8)	a)	(4.1)	50
5	(4.2)	(4.7)	b)	(4.1)	50
6	(4.2)	(4.5)	b)	(4.1)	50
7	(4.3)	(4.10)	a)	(4.1)	0.05
8	(4.2)	(4.10)	a)	(4.1)	50
9	(4.3)	- (4.10)	a)	(4.1)	0.05
10	(4.2)	- (4.10)	a)	(4.1)	50
11	(4.2)	(4.11)	a)	(4.1)	10
12	(4.2)	- (4.11)	a)	(4.1)	10
13	(4.3)	- (4.11)	a)	(4.1)	30
14	(4.3)	(4.11)	a)	(4.1)	30
15	(4.4)	(4.9)	c)	(4.4)	300

The Lamé constants were in all the examples fixed as $\lambda = 50\,, \mu = 100\,.$ For Example 6, we have also represented (in the last two figures entitled Section 1 and

Section 2) the deformation of the cross section in two points, corresponding to the division points $i = 50$ and $i = 100$. In all the examples, the interval $[T_1, T_2]$ on which $\bar{\theta}(\cdot)$ is defined was divided in 200 equal subintervals, i.e. $i = 50$ and $i = 100$ correspond to the first quarter and to the middle of the curved rod. The scalings used for the various figures are intended to obtain a clearer graphical representation, and the procedure is equivalent to the multiplication of the force by the given factor, due to the linearity of the equations. In the figures for Section 1 and Section 2, the scalings are 20, respectively 10. Notice that the shear and the torsion effects are not represented, since this would require 3D figures. Our aim in the numerical simulation was to test the modelling approach, and all experiments have produced meaningful results from a mechanical point of view. We have avoided the well-known "locking problem" appearing in the numerical approximation of arches, rods and shells, Chenais and Paumier [8], Arunakirinathar and Reddy [3], Chapelle [7], Pitkäranta and Leino [16], by choosing a very fine division of $[T_1, T_2]$ in comparison with the dimension of the cross sections, i.e. by taking "large" cross sections.

Consequently, we have used standard piecewise linear, continuous finite elements on $[T_1, T_2]$. If V_m, $m = 200$, is the discrete subspace associated to $H_0^1(T_1, T_2)$, then V_m^9 is associated to $H_0^1(T_1, T_2)^9$, and its finite element basis is constructed in a canonical way. The rigidity matrix is sparse, and the number of unknowns in the obtained linear algebraic system (corresponding to (2.32)) was 1791. The integrals over the cross sections, appearing in the coefficients, were computed by a change of variable to polar coordinates, which reduced all the cases to various rectangles and, then, by classical interpolation methods. Since the dimension was not very big, the algebraic linear system was solved by the Gaussian elimination method, which is known to be very stable. In all the computed examples, we have noticed that the vectors $\bar{N}^m\left(\frac{T_1+T_2}{2}\right)$ and $\bar{B}^m\left(\frac{T_1+T_2}{2}\right)$ (the deformations of the "normal" and "binormal" vectors, in the middle of the rod) are orthogonal.

Finally, we point out that, although the theoretical results allow variable cross sections, nonzero surface tractions, and not centered line of centroids (see (2.1)), these elements were not implemented in the numerical examples in order to keep the complexity of the computations at a reasonable level.

References

[1] J. A. Alvarez-Dios and J. M. Viaño, *An asymptotic bending model for a general planar curved rod*, in: Shells: mathematical modelling and scientific computing, M. Bernadou, P. G. Ciarlet and J. M. Viaño, Eds., Univ. Santiago de Compostela Press, Spain, 1997, pp. 11–17.

[2] S. S. Antman, *Nonlinear problems of elasticity*, Springer Verlag, Berlin, 1995.

[3] K. Arunakirinathar and B. D. Reddy, *Mixed finite element methods for elastic rods of arbitrary geometry*, Numer. Math., **64** (1993), pp. 13–43.

[4] A. Blouza and H. Le Dret, *Existence et unicité pour le modèle de Koiter pour une coque peu régulière*, CRAS Paris, t. **319** (1994), Série I, pp. 1127–1132.

[5] A. Blouza, *Existence et unicité pour le modèle de Nagdhi pour une coque pou régulière*, CRAS Paris, t. **324** (1997), Série I, pp. 839–844.

[6] H. Cartan, *Formes différentielles*, Hermann, Paris, 1967.

[7] D. Chapelle, *A locking-free approximation of curved rods by straight beam elements*, Numer. Math., **77** (1997), pp. 299–322.

[8] D. Chenais and J. C. Paumier, *On the locking phenomenon for a class of elliptic problems*, Numer. Math., **67** (1994), pp. 427–440.

[9] Ph. Ciarlet, *The finite element method for elliptic problems*, North-Holland, Amsterdam, 1978.

[10] Ph. Ciarlet, *Introduction to linear shell theory*, Gauthier-Villars, Paris, 1998.

[11] M. C. Delfour and Jiabin Zhao, *Intrinsic nonlinear models of shells*, CRM Proc. Lecture Notes, **21**, AMS (1999), pp. 109–123.

[12] A. Ignat, J. Sprekels and D. Tiba, *Analysis and optimization of non-smooth mechanical structures*, Preprint 581, Weierstrass Institute for Applied Analysis and Stochastics, Berlin, 2000, submitted to SICON.

[13] M. Jurak, J. Tambaca and Z. Tutek, *Derivation of a curved rod model by Kirchhoff assumptions*, ZAMM, **79** (1999), no. 7, pp. 455–463.

[14] J. E. Lagnese, G. Leugering and E. J. P. G. Schmidt, *Modeling, analysis and control of dynamic elastic multi-link structures*, Birkhäuser, Boston, 1994.

[15] F. Murat and A. Sili, *Comportement asymptotique des solutions du système de l'élasticité linéarisée anisotrope hétérogène dans les cylindres minces*, CRAS Paris, t. **328** (1999), Série I, pp. 179–184.

[16] J. Pitkäranta and Y. Leino, *On the membrane locking of the $h-p$ finite elements in a cylindrical shell problem*, Internat. J. Numer. Methods. Engrg., **37** (1994), no. 6, pp. 1053–1070.

[17] B. D. Reddy, *Mixed finite element methods for one-dimensional problems: a survey*, Questiones Mathematicae, **15** (1992), no. 3, pp. 233–259.

[18] J. Sprekels and D. Tiba, *Sur les arches lipschitziennes*, CRAS Paris, t. 331 (2000), Série I, pp. 179–184.

[19] L. Trabucho and J. M. Viaño, *Mathematical modelling of rods*, Handbook of numerical analysis, vol. IV, P. G. Ciarlet and J. L. Lions, Eds., Elsevier, Amsterdam, 1996, pp. 487–974.

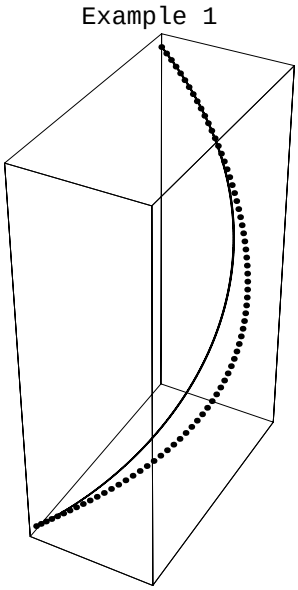

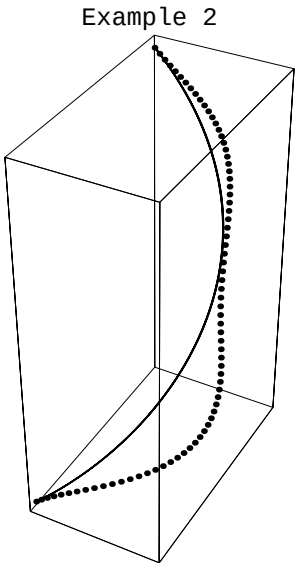

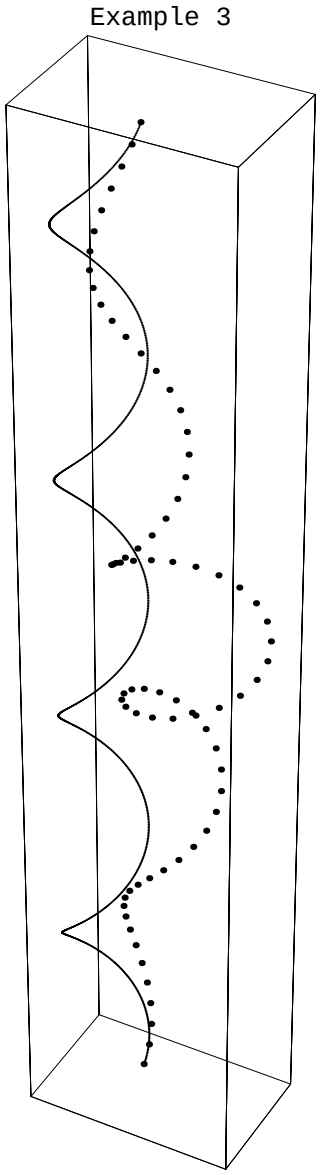

Example 4

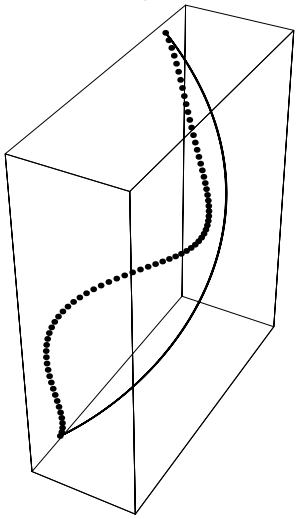

Example 5

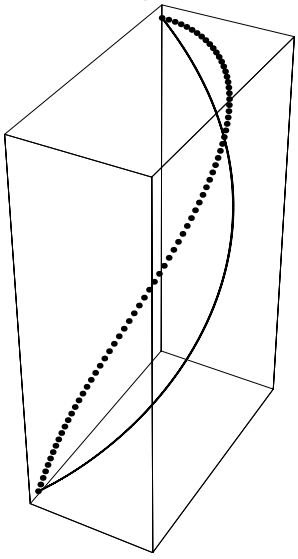

Example 6

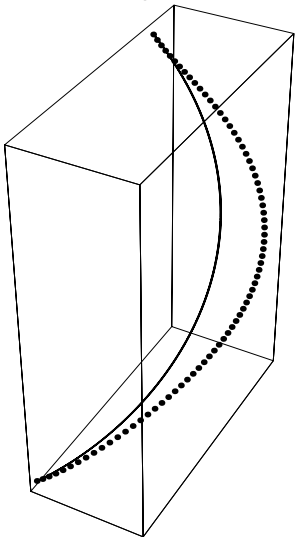

Example 7

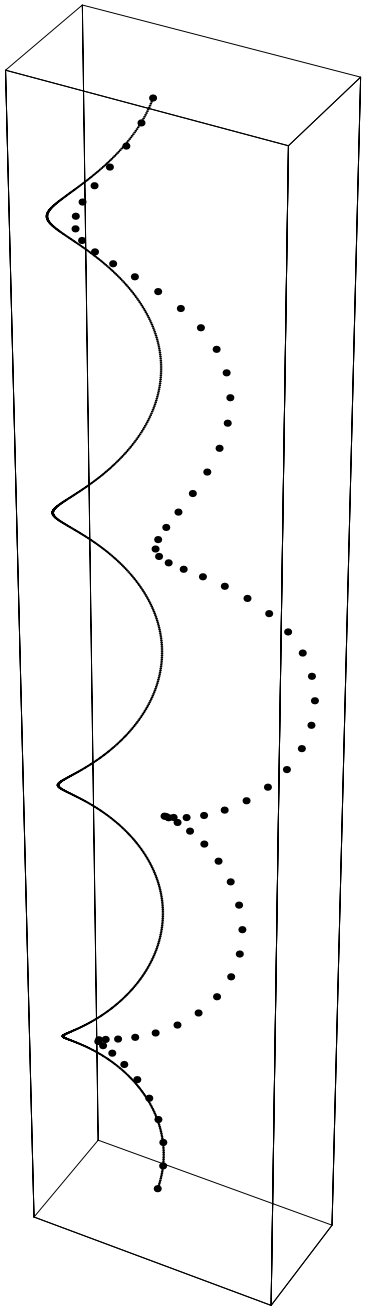

Example 8

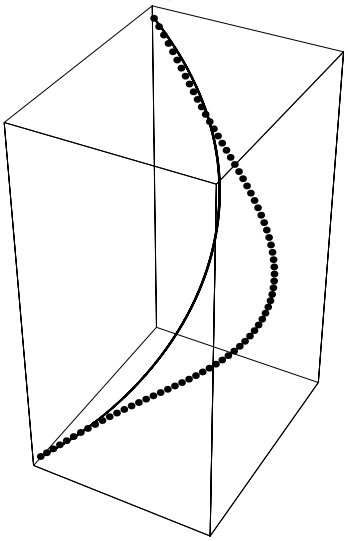

Example 9

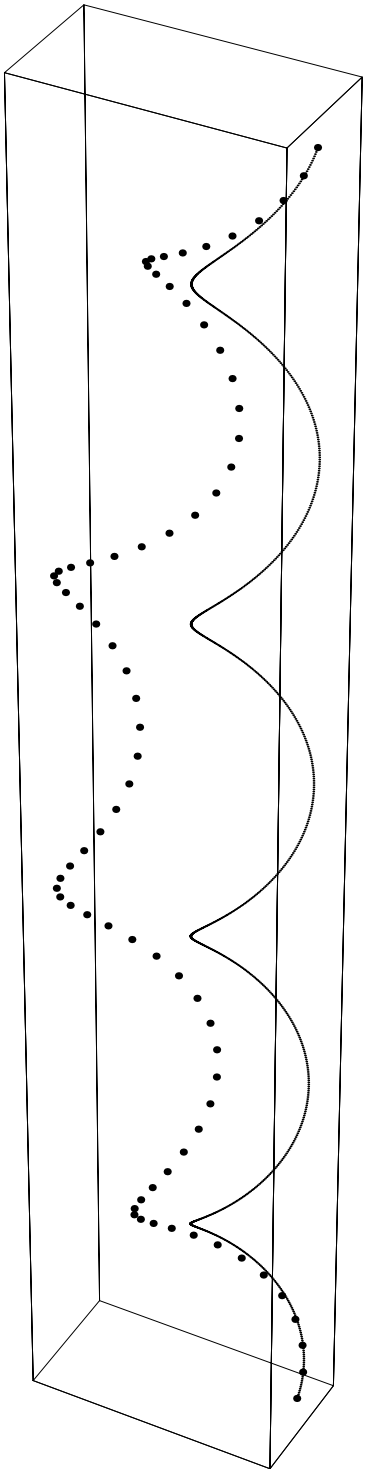

Example 10

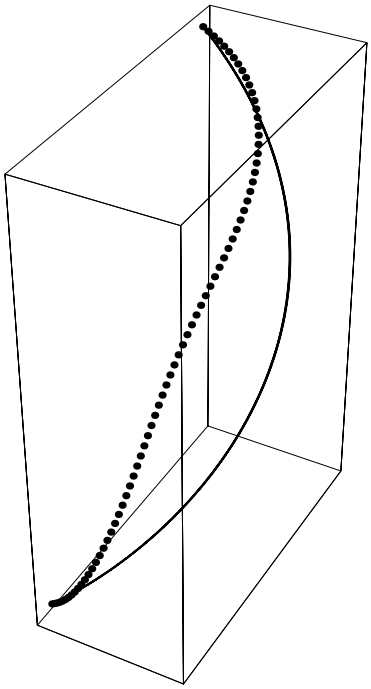

Example 11

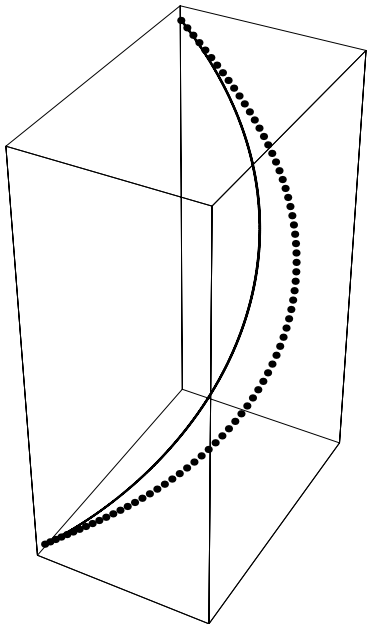

Example 12

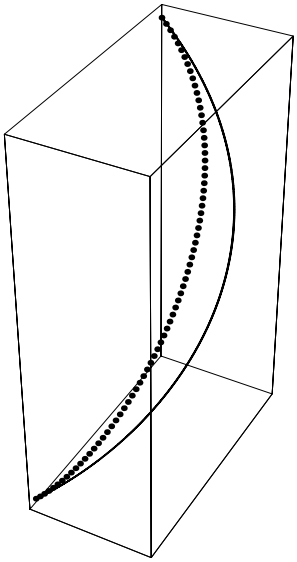

Example 13

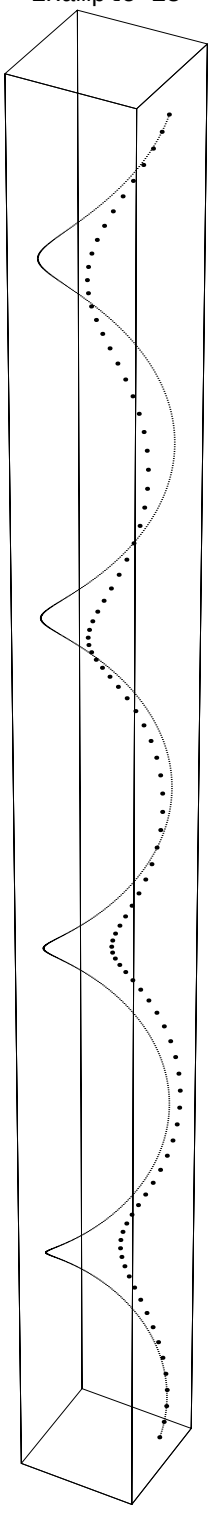

Example 14

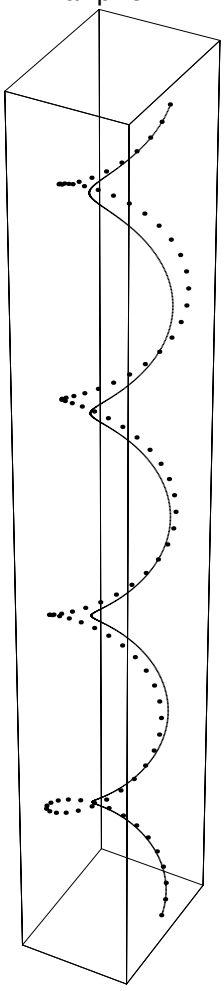

Example 15

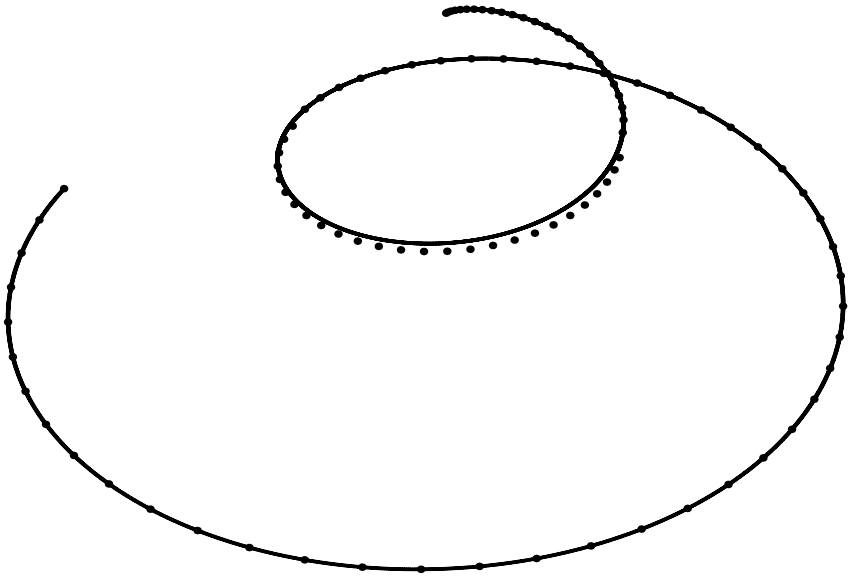

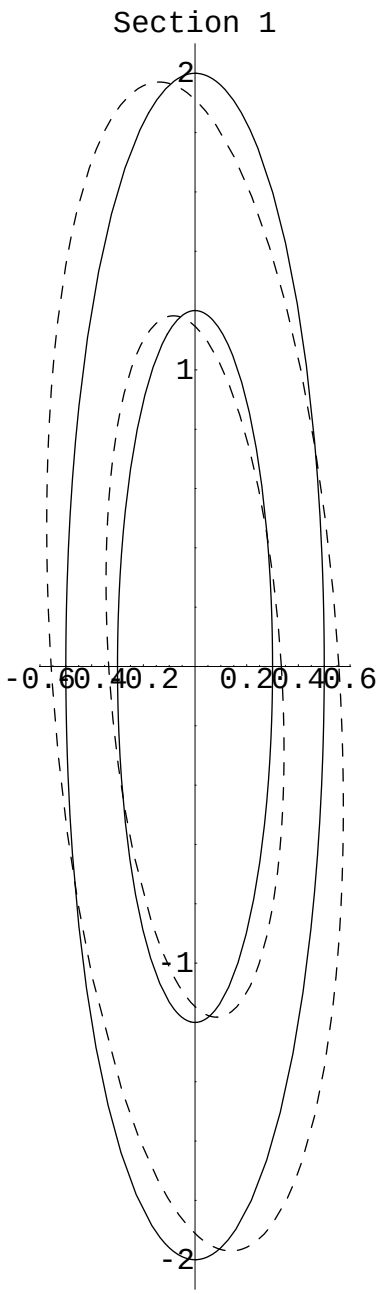
Section 1
2
1
-1
-2
-0.6
-0.4
-0.2
0.2
0.4
0.6

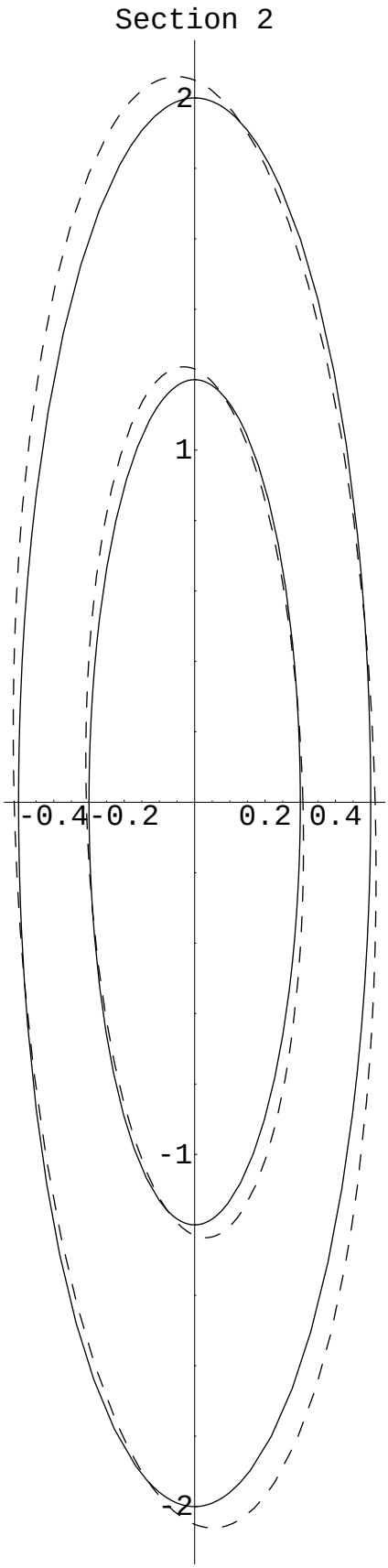
Section 2
2
1
-1
-2
-0.4
-0.2
0.2
0.4